

CONTRAST-INDEPENDENT CURVILINEAR STRUCTURE ENHANCEMENT IN 3D BIOMEDICAL IMAGES

Çiğdem Sazak and Boguslaw Obara

School of Engineering and Computing Science, Durham University, Durham, UK
boguslaw.obara@durham.ac.uk

ABSTRACT

A wide range of biomedical applications require detection, quantification and modelling of curvilinear structures in 3D images. Here we propose a 3D contrast-independent approach to enhance curvilinear structures based on the 3D Phase Congruency Tensor concept. The results show that the proposed method is insensitive to intensity variations along the 3D curve, and provides successful enhancement within noisy regions. The quality of the 3D Phase Congruency Tensor is evaluated by comparing it with state-of-the-art intensity-based approaches on both synthetic and real biological images.

Index Terms— Image enhancement, vesselness, neuriteness, Phase Congruency Tensor, 3D images.

1. INTRODUCTION

THE explosive growth in size and complexity of biomedical imaging data and the need for extracting quantitative information, increasingly requires sophisticated bioimage analysis methods. As a common requirement of strong and durable image enhancement, segmentation and analysing of curve-like features are essential in bioimaging. Accordingly, a significant number of image processing solutions has been propounded to enhance and extract 3D curve-like structures such as blood vessels. [1, 2], neurons [3], microtubules [4], and others as reviewed in [5]. Despite such a wide range of approaches, the robust enhancement of 3D curvilinear structures remains challenging due to the intensity variations along the 3D curve. To overcome this challenge, we propose a 3D contrast-independent approach to enhance curvilinear structures based on the Phase Congruency Tensor (PCT) concept [6]. Also, it will be shown that by replacing the Hessian tensor with PCT, we may actively reduce the dependence on local image contrast which has hampered other tensor-based methods. In particular, we show how the PCT concept may be used to improve standard 3D curvilinear feature measurement techniques, like vesselness and neuriteness.

2. RELATED WORK

2.1. 3D Intensity-based curve-like feature enhancement

2.1.1. Using tensors for local feature representation

The tensor representation of the local image structure almost provides the most information about how much the image

structures change through and across the dominant directions and, is generated by combining the outputs from polar separable quadrature filters [7]. Assume that an image $I(\mathbf{p})$, that $\mathbf{p} = [x, y, z]^T$ is a column vector representation of the 3D spatial location. A suitable notation of the local structure of the surface in the region of \mathbf{p} is given by the tensor defined as follows:

$$T = \sum_{\Theta} \|q_{\Theta}\|(\mathbf{u}_{\Theta}\mathbf{u}_{\Theta}^T), \quad (1)$$

where q_{Θ} is the output from an oriented quadrature filter and \mathbf{u}_{Θ} is the column vector in the direction Θ . In the 3D case, an orientation $\Theta = (\theta, \phi)$ can be specified by elevation θ and azimuth ϕ angles on a sphere of unit radius [8], and \mathbf{u}_{Θ} is the column vector:

$$\mathbf{u}_{\Theta} = \mathbf{u}_{\theta,\phi} = [\sin(\theta)\cos(\phi), \sin(\theta)\sin(\phi), \cos(\theta)]^T. \quad (2)$$

2.1.2. Scale space

Curvilinear features can be observed in various sizes and different scales in an image. The space scale representation is mostly used [2]. The essential idea is to insert the original image inside a group of progressively smoothed images, in which fine-scale details are successively suppressed. This approach is usually accomplished by the use of Gaussian filters, or their derivatives, with multiple scales obtained by varying the value of the variance.

For a given 3D image $I_{\sigma}(\mathbf{p})$ and given scale σ , the neighborhood of a point \mathbf{p} can be estimated by its first Taylor expansion:

$$I_{\sigma}(\mathbf{p} + \Delta\mathbf{p}) \approx I_{\sigma}(\mathbf{p}) + \Delta\mathbf{p}^T \nabla I_{\sigma}(\mathbf{p}) + \Delta\mathbf{p}^T H_{\sigma}(\mathbf{p}) \Delta\mathbf{p}, \quad (3)$$

where $H_{\sigma}(\mathbf{p})$ is the Hessian matrix, a tensor of second order partial derivatives of I at point \mathbf{p} and scale σ . In three dimensions, a spherical neighborhood met at the point \mathbf{p} is outlined by $H_{\sigma}(\mathbf{p})$ over an ellipsoid whose axes are along the eigenvectors $\mathbf{v}_{\sigma,i}$ of the Hessian and the respective semi-lengths are the magnitudes of the that eigenvalues $\lambda_{\sigma,i}$. Therefore, the detection of curvilinear structures can be performed by an analysis of the eigenvalues and eigenvectors. Two of the most well-known ways in this area that has been called vesselness and neuriteness.

3. METHODS

Our 3D extension of a 2D Phase Congruency Tensor (PCT) concept introduced by [6] is proposed here. The 3D PCT concept is then used to define 3D curvilinear feature enhancement techniques which are PCT vesselness and PCT neuriteness.

3.1. Orientation

In order to properly calculate the 3D phase congruency and our 3D PCT, a set of N points 3D orientations are defined using a concept of uniformly distributed points on the unit sphere. Such a distribution of all details can be found in [9]

3.2. 3D Phase-based detection

In terms of the local image phase approach that is contrast-independent curvilinear enhancement has been investigated by [10]. The calculation of local phases needs the use of quadrature pairs of filters to the image. Consequently, for a given image $I(\mathbf{p})$ and a quadrature pair of even $F_{s,\Theta}^e$ and odd $F_{s,\Theta}^o$ filters at scale s and orientation Θ , the response vector is given by its even and odd components $e_{s,\Theta}(\mathbf{p})$ and $o_{s,\Theta}(\mathbf{p})$:

$$[e_{s,\Theta}(\mathbf{p}), o_{s,\Theta}(\mathbf{p})] = [I(\mathbf{p}) * F_{s,\Theta}^e, I(\mathbf{p}) * F_{s,\Theta}^o]. \quad (4)$$

The amplitude of the s^{th} component is defined as:

$$A_{s,\Theta}(\mathbf{p}) = \sqrt{e_{s,\Theta}(\mathbf{p})^2 + o_{s,\Theta}(\mathbf{p})^2}, \quad (5)$$

and the local phase given by:

$$\varphi_{s,\Theta}(\mathbf{p}) = \text{atan} \left(\frac{o_{s,\Theta}(\mathbf{p})}{e_{s,\Theta}(\mathbf{p})} \right), \quad (6)$$

To implement phase enhancement, several quadrature filters have been proposed, especially the log-Gabor filter [11]

For our method, a 3D log-Gabor filter has been used. This is the one has two components and is obtained by multiplying the angular and radial components of the Gaussian transfer function on the logarithmic frequency domain [11]:

$$\hat{\mathcal{L}}(\omega, \Theta) = \exp \left(-\frac{\ln \left(\frac{\omega}{\omega_0} \right)^2}{2 \ln \left(\frac{\sigma_\omega}{\omega_0} \right)^2} \right) \cdot \exp \left(-\frac{\Theta^2}{2\sigma_\Theta^2} \right), \quad (7)$$

where ω_0 is central radial frequency of filter and σ_ω is the standard deviation controlling the filter bandwidth. Θ is the orientation of the filter and σ_Θ determines the angular spread.

3.3. Phase congruency

Phase congruency has been used to find a wide range of low-contrast features including step edges, line and roof edges [12]. The phase congruency design assumes that features are recognized at points where the Fourier components are

maximally in phase. In 3D, the phase congruency at several orientations is defined as [12]:

$$PC_{s,\Theta}(\mathbf{p}) = \sum_{\Theta} (PC_{\Theta}(\mathbf{p})), \quad (8)$$

and the phase congruency at each orientation Θ is defined as:

$$PC_{\Theta}(\mathbf{p}) = \frac{\sum_s w_{\Theta}(\mathbf{p}) \max(A_{s,\Theta}(\mathbf{p}) \Delta\Phi_{s,\Theta}(\mathbf{p}) - t, 0)}{\sum_s A_{s,\Theta}(\mathbf{p}) + \varepsilon}. \quad (9)$$

$A_{s,\Theta}(\mathbf{p})$ is the amplitude of the image component at the location \mathbf{p} through the use of a 3D log-Gabor filter with the scale s and orientation Θ . The t is a noise threshold and ε a factor that ensures against the division of zero [10]. The weight of frequency spread $w_{\Theta}(\mathbf{p})$ is defined as:

$$w_{\Theta}(\mathbf{p}) = \frac{1}{1 + \exp(\mu(b - l_{\Theta}(\mathbf{p})))}, \quad (10)$$

which penalizes frequency distributions that are expressly narrow. The parameters μ and b in this function are constants describing a gain factor and a cut-off value, respectively. A measure of filter response spread is defined as:

$$l_{\Theta}(\mathbf{p}) = \frac{1}{\aleph} \left(\frac{\sum_s A_{s,\Theta}(\mathbf{p})}{A_{\max}(\mathbf{p}) + \varepsilon} \right), \quad (11)$$

where \aleph is a total number of scales. Finally, a phase deviation $\Delta\Phi_{s,\Theta}(\mathbf{p})$ in Equation 9 is defined as:

$$\Delta\Phi_{s,\Theta}(\mathbf{p}) = e_{s,\Theta}(\mathbf{p})\bar{\varphi}_{s,\Theta}^e(\mathbf{p}) + o_{s,\Theta}(\mathbf{p})\bar{\varphi}_{s,\Theta}^o(\mathbf{p}) - |e_{s,\Theta}(\mathbf{p})\bar{\varphi}_{s,\Theta}^o(\mathbf{p}) - o_{s,\Theta}(\mathbf{p})\bar{\varphi}_{s,\Theta}^e(\mathbf{p})|, \quad (12)$$

where $\bar{\varphi}_{s,\Theta}^{\{e,o\}}(\mathbf{p}) = \sum_s \{e, o\}_{s,\Theta}(\mathbf{p})/E_{\Theta}(\mathbf{p})$, and

$$E_{\Theta}(\mathbf{p}) = \sqrt{\left(\sum_s e_{s,\Theta}(\mathbf{p}) \right)^2 + \left(\sum_s o_{s,\Theta}(\mathbf{p}) \right)^2},$$

where $E_{\Theta}(\mathbf{p})$ is the local energy and $\varphi_{s,\Theta}(\mathbf{p})$ is the cosine of the deviation of the phase while $\bar{\varphi}_{s,\Theta}(\mathbf{p})$ is the overall mean phase angle.

3.4. 3D PCT vesselness and 3D PCT neuriteness

3D piecewise curvilinear segments can be enhanced by analysing the relations between eigenvalues and eigenvectors of the 3D Hessian. In a similar way, using Equations 13 and 15, our 3D PCT-based vesselness and 3D PCT-based neuriteness are defined where the eigenvalues of 3D Hessian are substituted with those of the 3D PCT.

3.4.1. 3D vesselness

Vesselness as defined in [2] is computed as the ratio of the eigenvalues of $H_{\sigma}(\mathbf{p})$:

$$V_{\sigma} = \begin{cases} 0 & \lambda_{\sigma,2}, \lambda_{\sigma,3} < 0 \\ \exp \left(-\frac{R_{\beta}^2}{2\beta^2} \right) \left(1 - \exp \left(-\frac{R_{\alpha}^2}{2\alpha^2} \right) \right) \left(1 - \exp \left(-\frac{S^2}{2c^2} \right) \right) & \text{otherwise} \end{cases}, \quad (13)$$

where

$$S = \sqrt{\lambda_{\sigma,1}^2 + \lambda_{\sigma,2}^2 + \lambda_{\sigma,3}^2}, \quad R_\beta = \frac{|\lambda_{\sigma,1}|}{\sqrt{|\lambda_{\sigma,2}\lambda_{\sigma,3}|}}, \quad R_\alpha = \frac{|\lambda_{\sigma,2}|}{|\lambda_{\sigma,3}|},$$

where α , β and c are positive real user-defined parameters. The R_β ratio calculates blob-like features [2] and the R_α ratio helps to discriminate between plate-like and line-like structures [13]. S is equal to half of the maximum Frobenius norm and evaluates whether the eigenvalues are large compared to noise. Finally, multi-scale vesselness, for a given set of scales $\Sigma = \{\sigma_i\}$ and $i = 1, 2, 3, \dots$, can be calculated as [6]:

$$V_\Sigma = \max_{\sigma \in \Sigma} (V_\sigma). \quad (14)$$

3.4.2. 3D neuriteness

For the another Hessian matrix based method has been proposed by [14] for 2D and extended in [3] that is required second-order derivatives of the Gaussian Kernel with a given scale σ , for 3D as follows:

$$N_\sigma = \begin{cases} \frac{\lambda_{\sigma,max}}{\lambda_{\sigma,min}} & \lambda_{\sigma,max} < 0 \\ 0 & \lambda_{\sigma,max} \geq 0 \end{cases}, \quad (15)$$

where

$$\begin{aligned} \lambda_{\sigma,max} &= \max(|\lambda'_{\sigma,1}|, |\lambda'_{\sigma,2}|, |\lambda'_{\sigma,3}|), \\ \lambda_{\sigma,min} &= \min(\lambda_{\sigma,max}), \\ \lambda'_{\sigma,1} &= \lambda_{\sigma,1} + \gamma\lambda_{\sigma,2} + \gamma\lambda_{\sigma,3}, \\ \lambda'_{\sigma,2} &= \gamma\lambda_{\sigma,1} + \lambda_{\sigma,2} + \gamma\lambda_{\sigma,3}, \\ \lambda'_{\sigma,3} &= \gamma\lambda_{\sigma,1} + \gamma\lambda_{\sigma,2} + \lambda_{\sigma,3}. \end{aligned}$$

Parameter γ is chosen by 1/3 as in [3].

4. RESULTS

The performance of the 3D PCT-based methods for curvilinear structure detection was tested on a synthetic image (Figure 1), also real biological images of keratins and neuronal networks. A synthetic image was designed to simulate branching structures in a noisy environment. Grid lines with a width of 10 pixels were generated on a bright, constant background. To simulate a real-life scenario, Gaussian noise with the 18 SNR was added to the image. Figure 1 illustrate the comparison between 3D Hessian- and 3D PCT-based methods when applied to such a synthetic image. Finally, Figure 2 demonstrates the result of tested real images. and shows the result of the proposed 3D PCT-based methods by comparing with the traditional 3D Hessian-based versions.

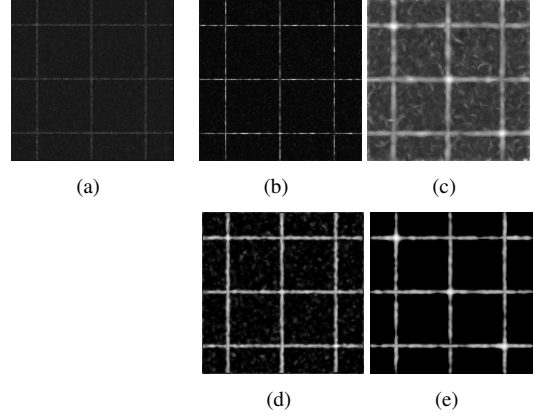


Fig. 1: Comparison between Hessian- and PCT-based approaches applied to a synthetic image (a): vesselness (b), neuriteness (c), PCT vesselness (d), and PCT neuriteness (e). 2D max projections of 3D images are shown.

5. CONCLUSION

Enhancement of the curvilinear structure is important for many biomedical applications. In this research we have proposed the 3D Phase Congruency Tensor concept used to define 3D contrast-independent curvilinear feature enhancement methods such as PCT vesselness and PCT neuriteness. Contrary of the 3D Hessian-based intensity-dependent methods, results indicated for the PCT-based approaches show a much higher degree of uniformity in the results, which greatly facilitates an accurate feature enhancement. Finally, the 3D PCT concept can be adapted to methods for finding other non-curvilinear structures such as junctions or ending points where high curvature values exist along more than one principal directions. Compare to traditional methods like vesselness and neuriteness, our proposed method resists to noisy background and also strong to enhance curve-like features in the bioimage. Other use of the 3D PCT concept in exchange for the 3D Hessian matrix could be in 3D anisotropic diffusion schemes [15] and 3D live-wire tracing methods [14].

6. REFERENCES

- [1] Fethallah Benmansour and Laurent D. Cohen, "Tubular structure segmentation based on minimal path method and anisotropic enhancement," *International Journal of Computer Vision*, vol. 92, no. 2, pp. 192–210, 2011.
- [2] Alejandro F Frangi, Wiro J Niessen, Koen L Vincken, and Max A Viergever, "Multiscale vessel enhancement filtering," in *Medical Image Computing and Computer-Assisted Intervention*, pp. 130–137, 1998.
- [3] Yousef Al-Kofahi, Natalie Dowell-Mesfin, Christopher Pace, William Shain, James N Turner, and Badrinath

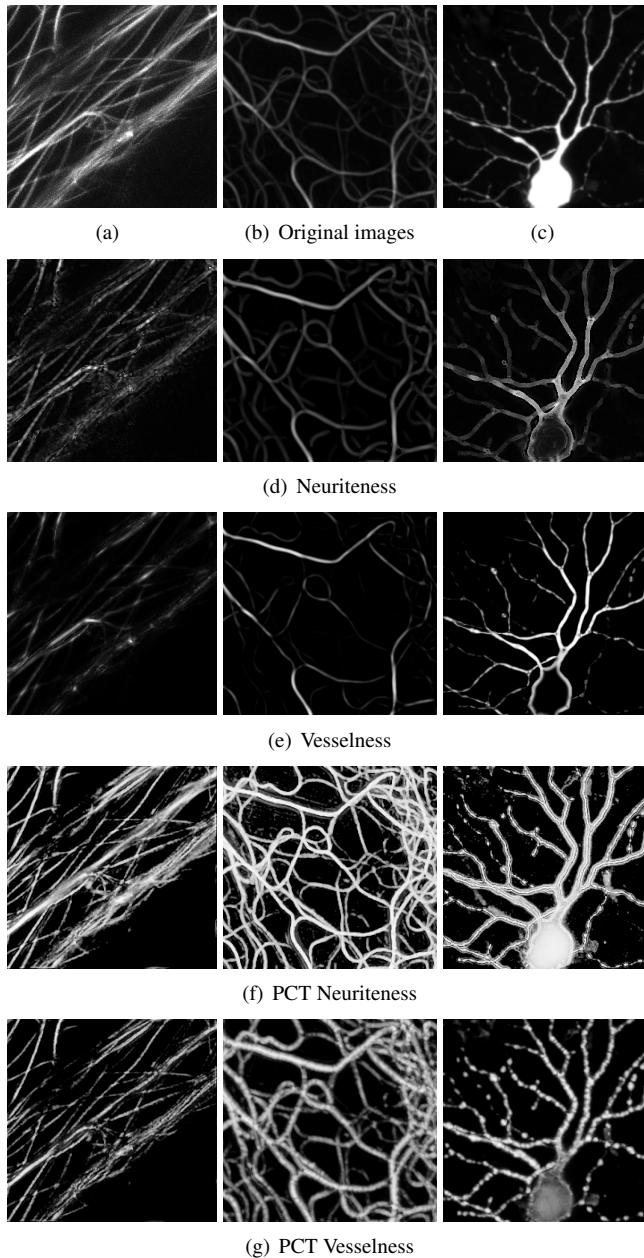


Fig. 2: 2D max projections of 3D images of microtubules network in a plant cell (a) and a keratin network in a skin cell (b) (Dr Tim Hawkins, Durham University, UK), and neuronal network (c) (Dr Chris Banna, UC Santa Barbara, USA). Comparison between Hessian- and PCT-based approaches applied to ROIs. Comparison approaches; neuriteness (d), vesselness (e), our methods; PCT neuriteness (f) and PCT vesselness (g).

Roysam, “Improved detection of branching points in algorithms for automated neuron tracing from 3D confocal images,” *Cytometry Part A*, vol. 73, no. 1, pp. 36–43, 2008.

[4] Stathis Hadjidemetriou, Derek Toomre, and James S Duncan, “Segmentation and 3D reconstruction of mi-

cro-tubules in total internal reflection fluorescence microscopy,” in *Medical Image Computing and Computer-Assisted Intervention*, pp. 761–769, 2005.

[5] David Lesage, Elsa D Angelini, Isabelle Bloch, and Gareth Funka-Lea, “A review of 3D vessel lumen segmentation techniques: Models, features and extraction schemes,” *Medical Image Analysis*, vol. 13, no. 6, pp. 819–845, 2009.

[6] Boguslaw Obara, Mark Fricker, David Gavaghan, and Vicente Grau, “Contrast-independent curvilinear structure detection in biomedical images,” *IEEE Transactions on Image Processing*, vol. 21, no. 5, pp. 2572–2581, 2012.

[7] H. Knutsson, “Representing local structure using tensors,” in *Scandinavian Conference on Image Analysis*, 19–22 June 1989, pp. 244–251.

[8] Ilker Hacihaliloglu, Rafeef Abugharbieh, Antony J Hodgson, and Robert N Rohling, “Enhancement of bone surface visualization from 3D ultrasound based on local phase information,” in *Ultrasonics Symposium*. IEEE, 2006, pp. 21–24.

[9] Edward B Saff and A BJ Kuijlaars, “Distributing many points on a sphere,” *The mathematical intelligencer*, vol. 19, no. 1, pp. 5–11, 1997.

[10] Peter Kovesei, “Image features from phase congruency,” *Journal of Computer Vision Research*, vol. 1, no. 3, pp. 1–26, 1999.

[11] Wei Wang, Jianwei Li, Feifei Huang, and Hailiang Feng, “Design and implementation of log-gabor filter in fingerprint image enhancement,” *Pattern Recognition Letters*, vol. 29, no. 3, pp. 301–308, 2008.

[12] Ricardo J Ferrari, Stéphane Allaire, Andrew Hope, John Kim, David Jaffray, and Vladimir Pekar, “Detection of point landmarks in 3D medical images via phase congruency model,” *Journal of the Brazilian Computer Society*, vol. 17, no. 2, pp. 117–132, 2011.

[13] Tim Jerman, Franjo Pernuš, Boštjan Likar, and Žiga Špiclin, “Beyond Frangi: An improved multiscale vesselness filter,” in *SPIE Medical Imaging*, 2015, pp. 94132A–94132A.

[14] E Meijering, M Jacob, J-CF Sarria, Pl Steiner, H Hirling, and M Unser, “Design and validation of a tool for neurite tracing and analysis in fluorescence microscopy images,” *Cytometry Part A*, vol. 58, no. 2, pp. 167–176, 2004.

[15] Boguslaw Obara, Mark Fricker, and Vicente Grau, “Coherence enhancing diffusion filtering based on the phase congruency tensor,” in *IEEE International Symposium on Biomedical Imaging*, 2012, pp. 202–205.